# Neutron diffraction and magnetocaloric effect studies of MnFe 1-x Co x P series of solid solutions

W. Chajec, Daniel Fruchart, R. Zach, J. Tobola, Mohamed Balli, E.K. Hlil, M. Artigas

# NEUTRON DIFFRACTION AND MAGNETOCALORIC EFFECT STUDIES OF $MnFe_{1-x}Co_xP$ SERIES OF SOLID SOLUTIONS

**W. CHAJEC[(a)], D. FRUCHART[(b)], R. ZACH[(a)], J. TOBOLA[(c)], M. BALLI[(d)], E.K. HLIL[(b)] and M. ARTIGAS[(e)]**

[(a)] Institute of Physics, Cracow University of Technology, 30-084 Cracow, Poland
wchajec@pk.edu.pl
[(b)] Institute Néel, CNRS, 38-042 Grenoble, BP 166X, France
[(c)] Faculty of Physics and Applied Computer Science, AGH, 30-059 Cracow, Poland
[(d)] University of Applied Sciences of Western Switzerland, Yverdon les Bains, Switzerland
[(e)] Depto Ciencia y Tecnología de Materiales y Fluidos, CPS and I.C.M.A. 50-015 Zaragoza, Spain

## ABSTRACT

$MnFe_{1-x}Co_xP$ intermetallic series of solid solutions ($0.4<x<0.6$) have been studied by means of powder neutron diffraction in 10−320 K temperature range. Rietveld analysis pointed out that $Co_2P$-type orthorhombic crystal structure (*SG*: *Pnma*) presents for all series. Helicoidal incommensurate antiferromagnetic structure with propagation vector $\boldsymbol{q}$ = [0, 0, q] were evidenced for all compounds at low temperature range. The $q$ value decreases with cobalt content and the second order polynomial q(x) it was evidenced, that is found well correlated with this dependence. Magnetic moments values of $\mu_{Mn}$=3.34 $\mu_B$ and $\mu_{(Fe,Co)}$=0.06 $\mu_B$ were determined from neutron diffraction refinements for x=0.4 at 10 K. In addition, magnetic interactions in relations with electronic band structure calculations of $MnFe_{1-x}Co_xP$ were presented and discussed reference to previous published data. Finally, magnetocaloric properties for selected compounds of the $MnFe_{1-x}Co_xP$ and $MnFe_{0.45}Co_{0.45}P_{0.9}Ge_{0.1}$ series of compounds are presented.

## 1. INTRODUCTION

Crystal structure and magnetic properties of the $MnFe_{1-x}Co_xP$ system appear strongly correlated in the vicinity of critical point as found in the *(x,T)* phase diagram (Figure.1) (Roger, 1970). The compounds of this system crystallize with the orthorhombic crystal structure of $Co_2P$-type (*SG:Pnma*). For $x<0.5$ and $T<250$K, the compounds exhibit antiferromagnetic (*AF*) properties only, whereas, for $x>0.5$, both antiferromagnetic-ferromagnetic (*AF-F*) and *F-P* phase transitions were evidenced in the *(x,T)* phase diagram (Roger 1970, Średniawa *et al.*, 2001, Zach *et al.*, 2007). The $T_{AF-F}$ phase transition temperature and the $T_C$ decreases and increases vs. the cobalt content, respectively. While $x>0.8$, the samples exhibit ferromagnetic properties and a very high $T_C$ was observed for MnCoP. Therefore, the increase of the cobalt content in the studied system causes the stabilization of the ferromagnetic state. The transitions exhibit magnetoelastic properties associated with the abrupt changes of lattice parameters and inducing the interatomic distances modification (Zach *et al.*, 2007).

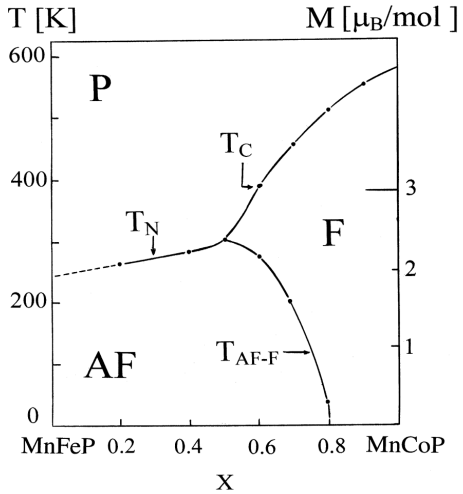


Figure 1. *(x,T)* magnetic phase diagram for $MnFe_{1-x}Co_xP$ (Roger 1970).

Electronic band structure calculations using the Korringa-Kohn-Rostoker method with the coherent potential approximation (KKR-CPA) (Bansil *et al.* 1999) were also performed (Średniawa *et al.*, 2001, Zach *et al.*, 2007). The density of states (DOS) at the Fermi level ($E_F$) and the magnetic moments versus cobalt concentration in the ferromagnetic state were calculated. It was clearly deduced that the ferromagnetic state was stable in the

region where DOS at $E_F$ shows the evidence of smaller values. Moreover for $MnFe_{0.7}Co_{0.3}P$, magnetic structure by means of KKR-CPA calculations was analyzed for different collinear models of *AF* state, enlightening important relations among magnetic interactions, local magnetic moments and magnetic ordering (Zach *et al*., 2007).

## 2. EXPERIMENTAL

The polycrystalline samples were synthesized starting from the appropriate amount of 99.9% pure elements. The fine powders of elements were mixed, then progressively heated up to 850°C for 8 days in evacuated silica tubes. The final heat treatment performed by high frequency heating allowed melting the sample before cooling it down. The quality of the samples was chequed by X-ray diffraction using Bragg-Brentano geometry ($\lambda_{Cu}$-$K_\alpha$ radiation). Neutron diffraction measurements for $MnFe_{1-x}Co_xP$ system (x=0.40, x=0.53, x=0.55 and x=0.60) in 10─320 K temperature range were carried at high flux reactor (ILL, Grenoble) by means of D1B spectrometer ($\lambda$=2.4 Å). The crystal structure and then magnetic structure determination were performed by using FullProf package (Rodrigues-Carvajal, 1993).

## 3. RESULTS AND DISCUSSION

Neutron diffraction patterns for a selected sample are reported in Figure. 2. The refinement procedure was started at the paramagnetic phase at high temperature. In this state the recorded spectra showed only nuclear maxima. Profile refinements were carried out within the *Pnma* space group (No. 62). All atoms occupy the same *4c* sites: (*x, ¼, z*), (*-x, ¾, -z*), (*1/2-x, ¾, ½+z*), (*1/2 +x, ¼, ½-z*), where *x* and *z* denote adjustable positional parameters. In the paramagnetic state, the pyramidal and tetrahedral sites occupancy by Mn, Co and Fe atoms, was analysed. The large difference among neutron scattering lengths for manganese ($b_{Mn}$=─3.73 fm), iron ($b_{Fe}$=9.45 fm) as well as cobalt ($b_{Co}$=2.49 fm) atoms was very helpful for the atom distribution analysis on the crystallographic sites. It was found that Mn atoms occupy exclusively pyramidal sites, whereas Co and Fe atoms are statistically distributed on tetrahedral sites. The crystal unit cell parameters i.e. lattice constants and (*x,z*) atomic positional parameters were also determined. Composition dependence of the unit cell volume measured at 10 K is presented in Figure. 3. These results remain in good agreement with the X-ray diffraction data recorded at room temperature (Roger, 1970). The small angle scattering maximum was found at low temperature range. It corresponds to incommensurate *AF* state (Figure. 4). Magnetic structure parameters previously found for the MnFeP (Chenevier, 1970, Suzuki *et al,* 1973), were used as initial parameters values for the $MnFe_{1-x}Co_xP$ series of solid solutions in our refinements (Figure 2). According to these authors it was assumed that magnetic moments of transition metal atoms localized in pyramidal (Mn) and tetrahedral (Fe, Co) sites lie in the *a-c* plane.

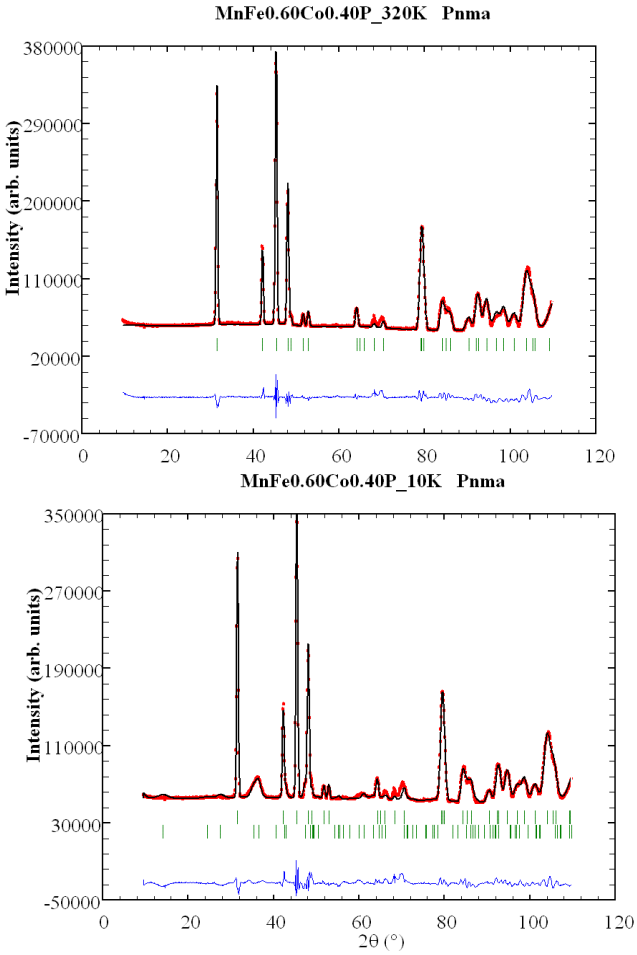


**Figure 2. Neutron diffraction pattern for $MnFe_{0.60}Co_{0.40}P$ recorded at 10K (AF). In the bottom spectra the difference diffraction patterns were placed. Vertical ticks indicate the positions of nuclear and/or magnetic reflections.**

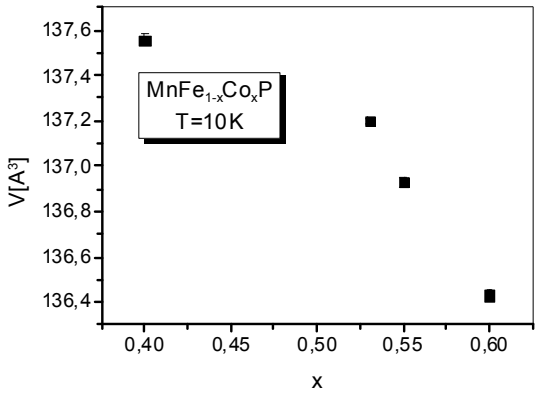


Figure 3. Concentration dependence of the V unit cell volume measured at 10K for the $MnFe_{1-x}Co_xP$.

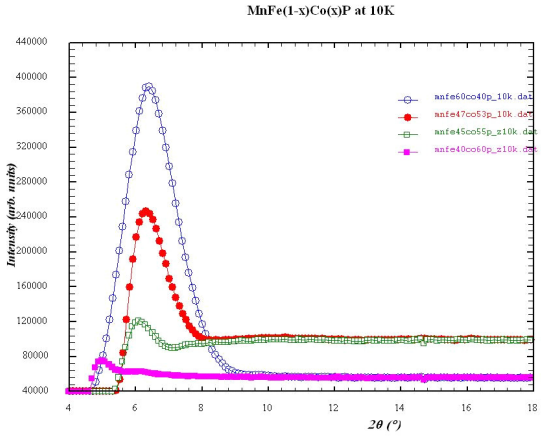


Figure 4. Variation of the small angle maxima (0,0,q(x)) recorded at 10 K for selected x cobalt contents.

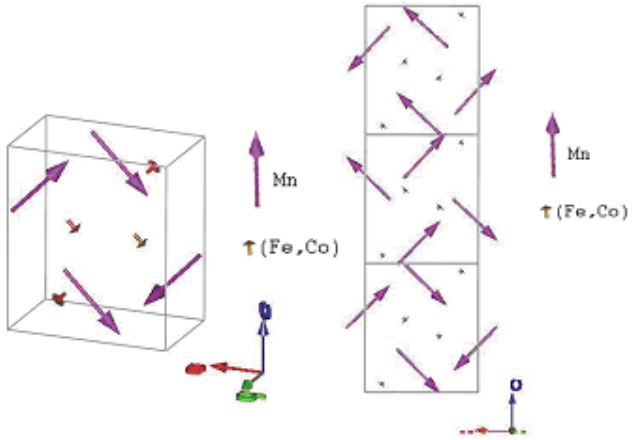


Figure 5. a) Mn and (Fe,Co) magnetic moments arrangement in the crystal unit cell; b) the Mn and the (Fe,Co) magnetic moments evolution in c direction.

Magnetic structure of helicoidal modulated type was determined in final refinement and the axis of the helicoida was established as directed along the *c* axis. As conclusion, the arrangements of magnetic moments located on both sites give evidence of magnetic order cycloida-type as seen in Figure 5 (Chajec *et al.*, 2008). Temperature dependence of magnetic moments localized on Mn and (Fe, Co) atoms are presented in Table 1. It points, that for $MnFe_{0.60}Co_{0.40}P$ magnetic moment localized on the manganese atoms is equal to $\mu_{Mn}=3.3\mu_B$. The Mn magnetic moment decreases very slowly with the increase of the cobalt content in the studied system. Simultaneously, it should be noticed, that magnetic moments on (Fe, Co) atoms localized on tetrahedral site are found to be significantly smaller than the Mn moment placed in the pyramidal one. The magnetic moment value in tetrahedral site increases versus cobalt content. The values of $\mu_{Mn}$ and $\mu_{(Fe,Co)}$ refined for compositions with x=0.40, x=0.53, x=0.55 and x=0.60 are collected in Table 1.

It is worth noting, that total magnetic moment on the tetrahedral site was determined as the average value of $\mu_{Fe}$ and $\mu_{Co}$. Temperature dependence of the propagation vector $\boldsymbol{q}$[0, 0, q] value is presented in Figure. 6 and listed in Table 1. Its value decreases versus temperature and x cobalt content. The second order polynomial *q(x)* fitted in the case of 10 K correlates quite well with the experimentally observed dependence. For $MnFe_{0.60}Co_{0.40}P$ as seen in Figure. 7, composition dependence of the interatomic distances at 10 K for $MnFe_{1-x}Co_xP$ system was also determined. It should be noticed, that good agreement between neutron and X-ray diffraction analysis was confirmed.

As known magnetic behaviour is directly related to electronic structure. For this reason electronic band structure calculations reported previously in the paper (Zach *et al.*, 2007) are recalled here, for better understanding of magnetic moments values on Mn, Fe and Co atoms, as well as their mutual arrangement. As aforementioned, the first principle calculations were based on the KKR-CPA allowing to account for the chemical disorder (Fe/Co) present on tetrahedral site. Comparison between the refined magnetic structure and the calculated models are highlighted. The calculated orderings both in the *F* and *AF* collinear magnetic states were analyzed. In this KKR-CPA computations, the helicoidal magnetic state was not considered since

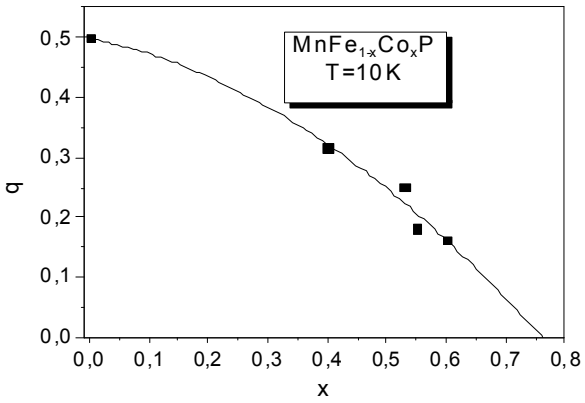


Figure 6.q propagation vector value vs. Co content calculated for 10 K.

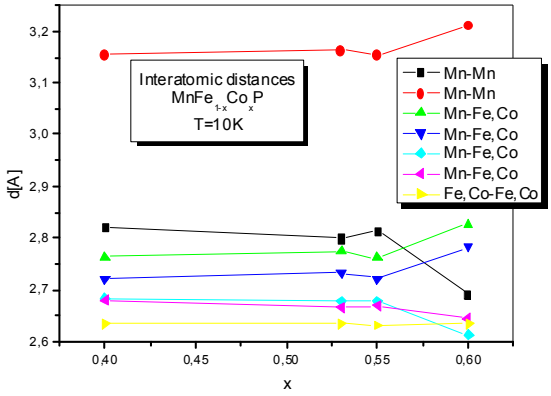


Figure 7. Composition dependence of the interatomic distances at 10 K in $MnFe_{1-x}Co_xP$.

Table 1. Values of magnetic moments localized in the pyramidal (Mn) and the tetrahedral (Fe,Co) sites for selected concentrations in $MnFe_{1-x}Co_xP$ system. The latter column concerns value of q propagation vector. The bottom line corresponds to ferromagnetic state. *AF-H* and *F* denote noncommensurate helimagnetic and ferromagnetic structures, respectively.

| x | | *T*/K | $\mu_{Mn}/\mu_B$ | $\mu_{(Co, Fe)}/\mu_B$ | *q* |
|---|---|---|---|---|---|
| **0.40** | *AF-H* | 10 | 3.34(7) | 0.06(9) | 0.3175(7) |
| | *AF-H* | 190 | 2.81(7) | 0.17(9) | 0.290(1) |
| **0.53** | *AF-H* | 10 | 3.30(8) | 0.23(9) | 0.253(1) |
| | *AF-H* | 190 | 2.53(8) | 0.51(9) | 0.231(1) |
| **0.55** | *AF-H* | 10 | 3.39(10) | 0.51(12) | 0.212(1) |
| | *AF-H* | 190 | 2.14(10) | 0.00(14) | 0.182(2) |
| **0.60** | *AF-H* | 10 | 3.21(14) | 0.74(18) | 0.163(1) |
| | *AF-H* | 190 | 2.57(14) | 0.84(15) | 0.134(3) |
| | *F* | 320 | 1.98(11) | 0.23(5) | - |

it was not easy to include it into this calculations (Zach *et al.*, 2007). Firstly, the site preference of Co and Fe atoms, located in the pyramidal and tetrahedral positions was analyzed and magnetic properties of Co and Fe sublattices were calculated based on total energy computations (Zach *et al.*, 2007). Particularly, these calculations well support the preference of the tetrahedral cobalt site for the iron impurity introduced in MnCoP. The electronic structure calculations of $MnFe_{1-x}Co_xP$ showed also that the disappearance of the *AF* state and the tendency to form the *F* state while increasing Co concentration. This behaviour is accompanied by a strong decrease in the total DOS at $E_F$ for x>0.6 (see ref. (Zach *et al.*, 2007)). This important drop in $N(E_F)$ is associated with only slight changes in magnetic moments. It is worth noticing that the magnetic moments calculated for MnCoP are in good agreement with previously reported neutron diffraction data ($\mu_{tot}$=3.03 $\mu_B$/f.u. from theory and 3.0 $\mu_B$/f.u. from experiment) (Zach *et al.*, 2007). Calculations, considering

different collinear *AF* models, performed only for x=0.3, revealed that *AF* coupling between Mn-Mn (inter) atoms plays a predominant role to decrease $N(E_F)$ with respect to *F* coupling. Furthermore, the shortest Mn-(Fe,Co) (inter) distances also seems to be important for stability of the magnetic state. The magnetic coupling type does practically not affect the calculated Mn magnetic moment values $\mu_{Mn}$≈2.95 $\mu_B$ (x=0.3), whereas small magnetic moments on Fe and Co atoms were found to be very sensitive to both inter-atomic distances between transition metals as well as to type of magnetic coupling.

Here, we have to keep in mind, that the calculations for the collinear *AF* state were carried out for x=0.3, whereas neutron diffraction experiments for helimagnetic state were performed for several other Co concentrations. However, the sample with the x=0.4 cobalt content, on which measurements were performed, the closest concentration (x = 0.3) for which calculation were proceeded. Magnetic moment on manganese atom, experimentally determined for x=0.4, as $\mu_{Mn}$≈3.3 $\mu_B$ and $\mu_{Mn}$≈ 2.8 $\mu_B$ at 10 K and 190 K were established, respectively (Table 1). The latter value remains in good agreement with calculated magnetic moment value $\mu_{Mn}$≈2.95$\mu_B$ for x=0.3 (note, that crystal structure parameters used in KKR-CPA calculations were determined at 100 K (Zach *et al.*, 2007). One remark should be made concerning averaged $\mu_{(Co,Fe)}$ magnetic moments localized on the tetrahedral site for x=0.4. As it is seen in the Table 1 the $\mu_{(Co,Fe)}$ ≈0.06 $\mu_B$ and $\mu_{(Co,Fe)}$ ≈ 0.17 $\mu_B$ at 10 K and 190 K were found, respectively. This is also in good agreement with the calculated weighted average value of Fe and Co magnetic moments for x=0.3 (KKR-CPA, (Zach *et al.*, 2007)).

Finally, we conclude that the small difference between the experimental and the calculated Mn and (Fe, Co) magnetic moment values may originate from the fact that the KKR-CPA computations considered only the collinear *AF* structure, whereas in reality the incommensurate helimagnetic structure was experimentally stated in course of this work.

At the end of this report we discuss the MCE in $MnFe_{1-x}Co_xP$ series of solid solutions. Magnetization experiments at the Institute Néel, CNRS, Grenoble at superconducting magnet (10 T) in 4.2─400 K temperature range were carried out. Both isothermal $M_T(B)$ and isofield $M_B(T)$ magnetization curves were recorded for selected compounds. The extraction method was used to measure the magnetization of the sample. The integration of the pick-up coil signals was performed by means of a voltage-frequancy converter and an integrating digital voltmeter. The temperature was measured by a platinum or carbon resistor placed outside of the sample holder but having metallic contact with it. The calorimeter enables good temperature control and regulation.

In the Figure. 8 for $MnFe_{0.2}Co_{0.8}P$ compound temperature dependence of the magnetic entropy changes is presented. Maximum value of entropy for the magnetic field jump of 1 T was found as equal to 0.5 J/Kkg. However in the case of magnetic field jump of 7 T magnetic entropy jump was estimated of about 3.5 J/Kkg.

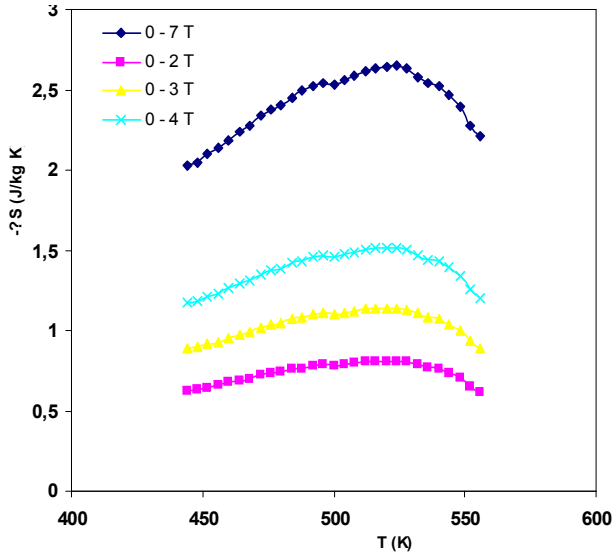


Figure 8. Temperature variation of magnetic entropy change for $MnFe_{0.2}Co_{0.8}P$ recorded at different magnetic field values.

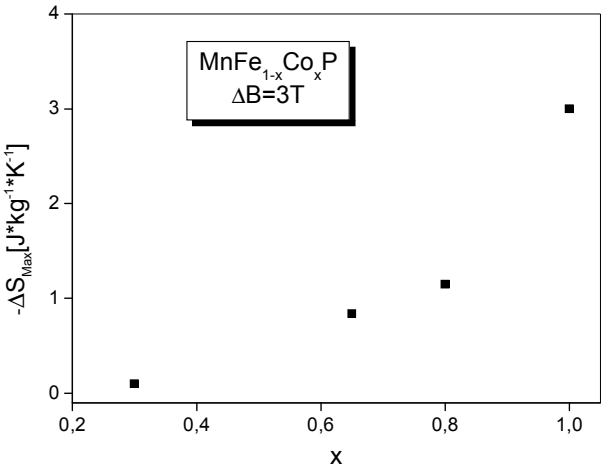


Figure 9. Composition dependence of magnetic entropy change at $T_N$(x=0.3) and $T_C$ (x=0.65, 0.8 and 1.0) for $MnFe_{1-x}Co_xP$ system.

Similar amplitude of MCE was found in the case of other concentrations. Composition dependence of $-\Delta S_m$ for selected contents is presented in the Figure. 9. It should be noticed that in the case of the $MnFe_{1-x}Co_xP$ system the MCE is rather weak but its value was found as increasing with cobalt concentraton. We suppose that the weak magnetoelastic character of the F-P phase transitions is the main reason of small MCE observed in this series of compounds. On the other hand, the MCE effect was also studied in the vicinity of the AF-F phase transition. The estimated value of magnetic entropy jump as 0.8J/kgK (x=0.65) was found.
In addition the $MnFe_{0.45}Co_{0.55}P_{0.9}Ge_{0.1}$ compound was measured under magnetic field to record $M_T(B)$ iso-temperature magnetization curves. Special attention for MCE analysis was paid to AF-F phase transition temperature. In Figure. 10 the evolution of $-\Delta S_m$ vs. temperature at different magnetic field values was presented. In conclusion we should underline that the presence of small amount of germanium changed character of the AF-F phase transition and the shape of $\Delta S_m$ curves. Furtheremore it should be noted, that in the case of the latter compound, the amplitude of MCE was found as clearly increased in comparison with all the samples with no germanium content.

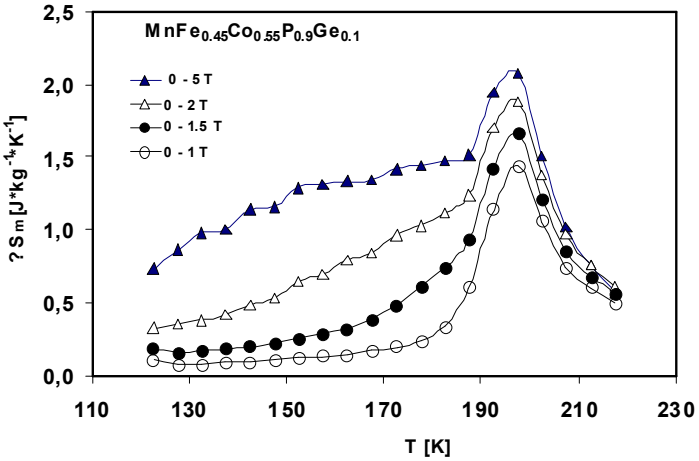


Figure 10. Temperature dependence of magnetic entropy change recorded at different field for the $MnFe_{0.45}Co_{0.55}P_{0.9}Ge_{0.1}$.

## 4. CONCLUSIONS

In this work, magnetic properties of the $MnFe_{1-x}Co_xP$ series of solid solutions, crystallizing for all compositions in $Co_2P$-type crystal structure, were presented. The following conclusions should be underlined:

1) The preference in sites occupation was observed. The Mn atoms occupy exclusively pyramidal sites, whereas Co and Fe atoms are randomly distributed in the tetrahedral positions, which remains in fair agreement with KKR-CPA total energy analysis (Zach *et al.*, 2007). A very good stoichiometry in the studied samples was established.

2) The magnetic ordering as the helicoidally modulated *AF* phase was proposed in all measured compounds (x=0.4, x=0.53, x=0.55 and x=0.60). It should be mentioned that in our case the incommensurate magnetic structure was determined.

3) A good agreement between the refined Mn, Co, Fe magnetic moments and the calculated ones by the KKR-CPA method was pointed out.

4) The systematic MCE studies in the $MnFe_{1-x}Co_xP$ series of compounds were undertaken both in the vicinity of the Curie temperature and the *AF-F* phase transition temperature. The systematic increase of the $\Delta S_m$ magnetic entropy jump versus cobalt concentration at $T_C$ was established. Contrary, the $\Delta S_m$ slightly decreases versus x cobalt content at the *AF-F* transition.

While 10% of germanium in the place of phosphorus was introduced in $MnFe_{1-x}Co_xP$ series, rather important increase of MCE amplitude associated with the *AF-F* was obtained.

## ACKNOWLEDGEMENTS

This work was supported under the Polish grant no. PO 3B 113 29, Polish-French cooperation project Polonium no 11609VG as well as by EFS European Project no UDA-POKL.04.01.01-00-001/08-00.

## REFERENCES

**Bansil A**, Kaprzyk S, Mijnarends PE and Tobola J. 1999, *Phys. Rev. B* 60:13373.
**Chajec W**, Zach R, Fruchart D, Toboła J, Balli M, Hlil EK and Artigas M. 2008, International Conference on Solid Compounds of Transition Elements, Dresden, July.
**Chenevier B**. 1990, *PhD. Thesis,* University of J. Fourier, Grenoble.
**Rodrigues-Carvajal J**. 1993, *Physica B* 192:55.
**Roger A**. 1970, *PhD. Thesis*, University of Paris.
**Suzuki T**, Yamaguchi Y, Yamamoto H and Watanabe H. 1973, *J. Phys. Soc. Jpn.* 34 :911
**Średniawa B**, Zach R, Fornal P, Duraj R, Bombik A, Toboła J, Kaprzyk S, Nizioł S, Fruchart D, Bacmann M, Fruchart R and Stanek J. 2001, *J. Alloys Comp*. 317–318:266.
**Zach R**, Tobola J, Średniawa B, Kaprzyk S, Guillot M, Fruchart D and Wolfers P. 2007, *J. Phys. Condens. Matter* 19:376201 (and references therein).